Infection with CagA^{+} *Helicobacter pylori* induces epithelial to mesenchymal transition in human cholangiocytes

Prissadee Thanaphongdecha[1,2,3], Shannon E. Karinshak[1], Wannaporn Ittiprasert[1], Victoria H. Mann[1], Yaovalux Chamgramol[3], Chawalit Pairojkul[3], James G. Fox[4], Sutas Suttiprapa[2], Banchob Sripa [2,3,*], Paul J. Brindley[1,*]

[1] Department of Microbiology, Immunology and Tropical Medicine, and Research Center for Neglected Tropical Diseases of Poverty, School of Medicine & Health Sciences, The George Washington University, Washington DC, 20037, USA

[2] Tropical Disease Research Laboratory, Faculty of Medicine, Khon Kaen University, Khon Kaen 40002, Thailand

[3] Department of Pathology, Faculty of Medicine, Khon Kaen University, Khon Kaen, 40002, Thailand

[4] Division of Comparative Medicine, Massachusetts Institute of Technology, Cambridge, 02139, MA

[*] Equal contribution

Correspondence: Paul J. Brindley, Department of Microbiology, Immunology and Tropical Medicine, and Research Center for Neglected Tropical Diseases of Poverty, School of Medicine & Health Sciences, The George Washington University, Washington DC, 20037, USA, email, pbrindley@gwu.edu; or Banchob Sripa, Tropical Disease Research Laboratory, Department of Pathology, Faculty of Medicine, Khon Kaen University, Khon Kaen 40002, Thailand, email, banchob@kku.ac.th

Abstract

Recent reports suggest that the East Asian liver fluke, *Opisthorchis viverrini*, infection with which is implicated in opisthorchiasis-associated cholangiocarcinoma, serves as a reservoir of *Helicobacter pylori*. The opisthorchiasis-affected cholangiocytes that line the intrahepatic biliary tract are considered to be the cell of origin of this malignancy. Here, we investigated interactions *in vitro* among human cholangiocytes, a CagA-positive strain of *Helicobacter pylori*, and the related bacillus, *Helicobacter bilis*. Exposure to increasing numbers of *H. pylori* at 0, 1, 10, 100 bacilli per cholangiocyte induced phenotypic changes including the profusion of thread-like filopodia and a loss of cell-cell contact, in a dose-dependent fashion. In parallel, following exposure to *H. pylori*, changes were evident in levels of mRNA expression of epithelial to mesenchymal transition (EMT)-encoding factors including snail, slug, vimentin, matrix metalloprotease, zinc finger E-box-binding homeobox, and the cancer stem cell marker CD44. Transcription levels encoding the cell adhesion marker CD24 decreased. Analysis to quantify cellular proliferation, migration and invasion in real time using the xCELLigence approach revealed that exposure to ≥10 *H. pylori* stimulated migration and invasion by the cholangiocytes through an extracellular matrix. In addition, 10 bacilli of CagA-positive *H. pylori* stimulated contact-independent colony establishment in soft agar. These findings support the hypothesis that infection with *H. pylori* contributes to the malignant transformation of the biliary epithelium.

Keyword : *Helicobacter pylori*, cholangiocyte, epithelial-to-mesenchymal transition.

Introduction

There is increasing evidence that the East Asian liver fluke *Opisthorchis viverrini* may serve as a reservoir of *Helicobacter* which, in turn, implicates *Helicobacter* in pathogenesis of opisthorchiasis-associated cholangiocarcinoma (CCA) [1-5]. The International Agency for Research on Cancer of the World Health Organization classifies infection with the liver flukes *O. viverrini* and *Clonorchis sinensis* as well as *H. pylori* as Group 1 carcinogens [6]. In northern and northeastern Thailand and Laos, opisthorchiasis is the major documented risk factor for CCA [6-9]. Given the elevated prevalence of CCA in this region where infection with liver fluke prevails, and given evidence of linkages between infection by *Helicobacter* during opisthorchiasis, these two biological carcinogens together may orchestrate the pathogenesis of opisthorchiasis and bile duct cancer. Indeed, it has been hypothesized that the association of *Helicobacter* and its virulence factors, including during opisthorchiasis, underlies much biliary tract disease including CCA in liver fluke-endemic regions [10]. Infection with species of *Helicobacter* causes hepatobiliary disease that can resemble opisthorchiasis [5, 11-14]. Lesions ascribed to liver fluke infection including cholangitis, biliary hyperplasia and metaplasia, periductal fibrosis and CCA may be, in part, *Helicobacter*-associated hepatobiliary disease.

With respect to the gastric epithelium and the association with stomach adenocarcinoma, *H. pylori* colonizes the mucosal layer [6], adheres to the epithelium through bacterial adhesins with cellular receptors [15], from where its virulence factors stimulate a cascade of inflammatory signaling, anti-apoptosis, cell proliferation and transformation pathways by its virulence factors [16-18]. Fox and coworkers were the first to speculate that *H. pylori* also can cause hepatobiliary diseases in humans [19]. This is the dominant species among the genus *Helicobacter* detected in the context of hepatobiliary disease [20] and *H. pylori* is detected more frequently in cases with CCA or hepatocellular carcinoma (HCC) than in those with benign tumors and other control groups [21, 22], suggesting a positive correlation between *H. pylori* infection and hepatic carcinogenesis. In addition to the extensive literature on the interactions between *H. pylori* and gastric cells [17, 23], interactions between biliary epithelium and this bacillus have been reported. Among these, *in vitro* studies revealed that *H. pylori* induces multiple effects in CCA cell lines, including inflammation (IL-8 production), cell proliferation and apoptosis. Even at low multiplicity of infection, *H. pylori* induces pro-inflammatory cytokine and cell proliferative responses in CCA cell lines [4, 24], and even small numbers of bacilli that likely reach the biliary tract routinely may be sufficient to promote inflammation and transformation of the biliary epithelia [24].

Commensalism involving *H. pylori* and *O. viverrini* may have evolved and may facilitate conveyance of the bacillus into the biliary tract during the migration of the juvenile fluke following ingestion of the metacercaria in raw or undercooked cyprinid fish and establishment of liver fluke infection [1, 25]. Since curved rods resembling *Helicobacter* have been documented in the digestive tract of *O. viverrini* [1] and, given the low pH of the gut of the fluke, the *H. pylori* rods or spores might be transported from the stomach to the duodenum by the migrating larval parasite. The curved, helical *H. pylori* rod attaches to a cholangiocyte, which internalize in similar fashion to its colonization of mucous-producing cells of the gastric epithelia [17, 26, 27].

Transition of epithelial cells to mesenchymal cells during disease and epithelial to mesenchymal transition (EMT) during development and wound healing follow evolutionary conserved routes with well-characterized morphological and other phenotypic hallmarks [28]. These phenotypes are showcases during malignant transformation of the gastric mucosa resulting from infection with *H. pylori* [29]. Here, we investigated interactions between CagA$^+$ *H. pylori*, the related species *H. bilis* [30], and human cholangiocytes. Infection with CagA$^+$ *H. pylori* induced EMT in the H69 cell line of human cholangiocytes [31, 32].

Materials and Methods

Cell lines of human cholangiocytes

The immortalized intrahepatic cholangiocyte cell line, H69 [31, 32], Cellosaurus [33] identifier RRID:CVCL_812,1, and the primary cholangiocarcinoma cell line, CC-LP-1 [34, 35] Cellosaurus RRID CVCL_0205, were obtained as described [34-37]. In brief, H69 cells were cultured in Dulbecco's Modified Eagle's Medium (DMEM) (Thermo Fisher Scientific, Inc.), DMEM/F12 (Millipore-Sigma, St. Louis, MO) supplemented with 10% fetal bovine serum (FBS)(Invitrogen, Thermo Fisher Scientific, Inc.) and adenine, insulin, epinephrine, triiodothyronine/transferrin, hydrocortisone, epidermal growth factor and penicillin/streptomycin (all from Millipore-Sigma), as described [36]. CC-LP-1 cells were cultured in DMEM containing 10% FBS, L-glutamine and penicillin/streptomycin. Both cell lines were maintained at 37°C in humidified 5% CO_2 in air. The cells were cultured to ~80% confluence before co-culture with *H. pylori*. H69 cells at passages 10 to 22 only and CC-LP-1 cells at passages 5 to 10 were used in this study.

Helicobacter pylori and *Helicobacter bilis*

Helicobacter pylori, ATCC 43504, from human gastric antrum [38], and *H. bilis*, Fox *et al.* ATCC 49314, from intestines and liver of mice [39, 40], were obtained from the American Type Culture Collection (ATCC) (Manassas, VA) and maintained under a microaerobic atmosphere on trypticase soy agar with 5% sheep blood for 72 to 96 hours [41] (Becton Dickinson, Cockeysville, MD), incubated at 37°C with gentle agitation in a microaerobic atmosphere, established with the BBL Campy Pack Plus system (Becton Dickinson). After 96 hours, each species of *Helicobacter* was harvested by scraping the colonies from the agar plate, and resuspension of the scraping in DMEM/F12 medium until an optical density at 600 nm of 1. 0 was reached, which corresponds to ~1×10^8 colony forming units (cfu)/ml [42-44]. Viability of the bacteria was confirmed by visual inspection for bacterial movement.

Morphological assessment of cholangiocytes

H69 cells were co-cultured with *H. pylori* at increasing multiplicities of infection (MOIs) of 0 (no bacilli), 10 and 100 for 24 hours in serum-free media. After 24 hours, the morphology of the H69 cells was documented and images captured using a digital camera fitted to an inverted microscope (Zeiss Axio Observer A1, Jena, Germany).

Cell scattering and elongation

184
185 H69 cells were seeded at 5 x 10^5 cells/well in 6-well culture plates (Greiner Bio-One, Monroe
186 NC). At 24 hours, the culture medium was exchanged for serum- and hormone-free medium
187 containing *H. pylori* at MOI of 0, 10, and 100, respectively, and maintained for a further 24
188 |hours. At that interval, the appearance including scattering of the cells in the cultures was
189 documented , as above. Cell scattering was quantified by counting the total number of isolated,
190 single cells per field in 10 randomly selected images at 5x magnification [45]. To assess
191 elongation of cells, images were documented of the cells in ~20 randomly selected fields of view
192 at ×20 magnification, with two to seven cells per field. The length to width ratio of the isolated
193 cells was established using the ImageJ software [46].
194
195 ***In vitro* wound healing assay**
196
197 Monitoring cell migration in a two-dimensional confluent monolayer may facilitate
198 characterization the process of wound healing with respect with exposure to *H. pylori* [47]. A
199 sheet migration approach was used to assay wound closure [36, 48, 49] following exposure of
200 the cholangiocytes to *H. pylori*. H69 cells infected with *H. pylori* at MOI of 0, 10 and 100 were
201 cultured overnight in 6-well plates to allow cell adherence. A linear scratch to wound the
202 monolayer was inflicted with a sterile 20 µl pipette tip. The dimensions of wound were
203 documented at 0 and at 26 hours, and the rate of wound closure quantified by measurement of
204 the width of the wound in the experimental and the control (MOI of 0) groups of cells [36, 37].
205
206 **Real time quantitative PCR (RT-qPCR)**
207
208 Total RNAs from H69 cells were extracted with RNAzol (Molecular Research Center, Inc.,
209 Cincinnati, OH) according to the manufacturer's instructions. The RNA Quantity and quality of
210 the RNAs were established by spectrophotometry (NanoDrop 1000, Thermo Fisher Scientific).
211 Total RNAs (500 ng) were reversed-transcribed using the iScript cDNA Synthesis Kit (Bio-Rad,
212 Hercules, CA). Analysis of expression of six EMT-associated genes - vimentin, snail, slug,
213 ZEB1, JAM1 and MMP7, and two cancer stem cell markers, CD44 and CD24 - was undertaken
214 by quantitative reverse transcription-polymerase chain reaction (qRT-PCR) of total RNAs using
215 an ABI7300 thermal cycling system (ABI) and the SsoAdvance SYBR green mixture (Bio-Rad).
216 Signals were normalized to expression levels for GAPDH. The relative fold-change was
217 determined by the ΔΔCt method [50]. Three biological replicates of the assay were undertaken.
218 Table S1 provides the oligonucleotide sequences of the primers in the RT-qPCRs. The design of
219 these primers for the human EMT and stem cell markers was undertaken used Primer- BLAST,
220 https://www.ncbi.nlm.nih.gov/tools/primer-blast/index.cgi [51], with the genome of *Helicobacter*
221 specifically excluded during the blast search. Further, before the RT-qPCR analysis was
222 undertaken, conventional PCR was carried out using cDNA from H69 cells as the template along
223 with these primers. Products were sized using ethidium bromide-stained agarose gel
224 electrophoresis, which confirmed that the presence of amplicons of predicted sizes (not shown).
225
226 **Assessment of cell proliferation**
227
228 Cell proliferation of H69 was assessed using the xCELLigence real-time cell analyzer (RTCA)
229 DP system (ACEA Biosciences, San Diego CA), as described [36, 52-54]. H69 cells were fasted

230 for 4 to 6 hours in 1:20 serum diluted medium, 0.5% FBS final concentration, as described [55,
231 56], after which cells were co-cultured of viable bacilli of *H. pylori* for 120 min before starting
232 the assay. H69 cells were subsequently harvested in 0.25% trypsin-EDTA and then washed with
233 medium. Five thousand H69 cells were seeded on to each well of the E-plate in H69 medium and
234 cultured for 24 hours. The culture medium was removed, and the cells were gently washed with
235 1×PBS. The PBS was replaced with serum diluted medium (above). The cellular growth was
236 monitored in real time with readings collected at intervals of 20 minutes for ≥ 60 hours. For
237 quantification, the cell index (CI) [53] was averaged from three independent measurements at
238 each time point.
239
240 **Cell migration and invasion in response to *H. pylori***
241
242 To monitor the rate of cell migration and/or invasion in real time, we used the xCELLigence DP
243 instrument (above) equipped with a CIM-plate 16 (Agilent ACEA Biosciences, San Diego CA),
244 which is an electronic Boyden chamber consisting of a 16-well culture plate in which each well
245 includes an upper chamber (UC) and a lower chamber (LC) separated by a microporous (pore
246 diameter, 8 μm) membrane. In response to a chemoattractant, cells may migrate/invade from the
247 UC towards the membrane and the LC. Migrating cells contact and adhere to microelectronic
248 sensors on the underside of the membrane that separates the UC from the LC, leading to change
249 in relative electrical impedance [53, 54, 57]. To investigate migration, H69 and CC-LP-1 cells
250 were infected with *H. pylori* at MOIs of 0, 1, 10, 50 and 100 respectively for 120 min before the
251 start of the assay, after which the cells were harvested following treatment for 3 min with 0.25%
252 trypsin-EDTA and washed with medium. Subsequently, 30,000 H69 or CC-LP-1 cells were
253 seeded into the UC of the CIM-plate in serum-free medium. Complete medium (including 10 %
254 FBS) was added to the LC. Equilibration of the loaded CIM-plate was accomplished by
255 incubation at 37°C for 60 min to allow cell attachment, after which monitoring for migration
256 commenced in real time for a duration of ~96 hours with readings recorded at 20 min intervals.
257 For quantification, CI was averaged from three independent measurements at each time point
258 [58].
259
260 To investigate invasion, H69 or CC-LP-1 cells were infected with *H. pylori* at either MOI of 0 or
261 10 at 120 minutes before commencing the t assay. The base of the UC of the CIM plate was
262 coated with 20% solution of a basement membrane matrix (BD Matrigel, BD Biosciences, San
263 Jose, CA) in serum-free medium. A total of 30,000 of H69 or CC-LP-1 cells were dispensed into
264 the UC in serum-free medium. The LC was filled with H69 or CC-LP-1 medium, as appropriate,
265 containing 10% FBS. The loaded CIM-plate was sealed, inserted into the RTCA DP
266 xCELLigence instrument at 37° C in 5% CO_2 and held for 60 min to facilitate attachment of the
267 cells, after which electronic recording was commenced. Monitoring for invasion in real time
268 continued for ~96 hours with the impedance value recorded at intervals of 20 min continuously
269 during the assay. CI was quantified as above.
270
271 **Colony formation in soft agar**
272
273 For the soft agar assay, H69 cells were infected with *H. pylori* or *H. bilis* at MOI of 0, 10, 50 and
274 100 at the start of the assay. H69 cells at 10,000 cells per well were mixed with 0.3% low
275 melting temperature agarose (NuSieve GTG) (Lonza, Walkersville, MD) in complete medium,

276 and plated on top of a solidified layer of 0.6% agarose in growth medium, in wells of 6- or 12-
277 well culture plates (Greiner Bio-One). Fresh medium was added every three or four days for 28
278 days or until the colonies had established, at which time the number of colonies of ≥ 50 μm
279 diameter was documented using a camera fitted to an inverted microscope (above) and quantified
280 [59].
281
282 **Statistical analysis**
283
284 Differences in cell elongation, cell scattering, wound healing and colony formation among
285 experimental and control groups were analysed by one-way analysis of variance (ANOVA). Fold
286 differences in mRNA levels, and real time cell migration and invasion through extracellular
287 matrix were analysed by two-way ANOVA followed by Dunnett's test for multiple comparisons.
288 Three or more replicates of each assay were carried out. Analysis was accomplished using
289 GraphPad Prism v7 (GraphPad, San Diego, CA). A P value of ≤ 0.05 was considered to be
290 statistically significant.
291
292 **Results**
293
294 ***Helicobacter pylori* induces epithelial to mesenchymal transition in cholangiocytes**
295
296 H69 were directly exposed to increasing number of *H. pylori* at 0, 10 and 100 bacilli per
297 cholangiocyte in 6-well plates. At 24 hours after addition of the bacilli, the normal epithelial cell
298 appearance in tissue culture had altered to an elongated phenotype characterized by terminal
299 thread-like filopodia and diminished cell-to-cell contacts (Figure 1A-C). The extent of the
300 transformation was dose-dependent and, also, it indicated increased cell motility. The
301 morphological change was quantified by measurement of the length to width ratio of the exposed
302 cells. In a dose dependent fashion, the ratio increased significantly at both MOI of 10 and of 100
303 when compared with MOI of 0, $P \leq 0.01$ (Figure 1D-F). In addition, the numbers of isolated,
304 single cells increased significantly to the increasing length to width ratio of the *H. pylori*-
305 exposed cholangiocytes, $P \leq 0.05$ and ≤ 0.001 at MOI of 10 and 100, respectively (Figure 1G).
306 The cholangiocytes displayed had a hummingbird phenotype-like appearance, reminiscent of
307 AGS gastric line cells [29]. Moreover, compared to H69 cells cultured in medium supplemented
308 with TGF-β at 5 ng/ml displayed cell aggregation and nodule formation (Figure S1).
309
310 **EMT-associated-factors induced by exposure to *H. pylori***
311
312 Transcriptional dynamics of the apparent EMT was investigated using qRT- PCR of total cellular
313 RNAs for six EMT-related factors including the mesenchymal marker vimentin, the transcription
314 factors, Snail, Slug and ZEB1, the adhesion molecule JAM1 and the proteolytic enzyme, MMP7
315 [60-62]. The cancer stem cell markers, CD24 and CD44 [63] also were monitored. Levels of the
316 fold-difference in transcription for each of the six markers increased in a dose-dependent fashion.
317 The regulatory transcriptional factor, Snail was markedly up-regulated with highest level of fold
318 difference, 88-, 656- and 5,309-fold at MOI of 10, 50 and 100, respectively, followed by MMP7,
319 with 15-, 21-, and 44-fold at MOI of 10, 50 and 100, respectively. Transcription of Slug, ZEB1,
320 vimentin and JAM1 also was up-regulated during bacterial infection. CD24 expression was
321 down-regulated whereas CD44 was up-regulated, revealing a $CD44^{+}$ high/$CD24^{+}$ low phenotype

322 in cells exposed to *H. pylori* (Figure 2; $P \leq 0.05$ to ≤ 0.0001 for individual EMT markers and/or
323 MOI level, as shown). A pattern of $CD44^+$ high/$CD24^+$ low expression is a cardinal character of
324 cancer stem cell activity in gastric adenocarcinoma [63].
325
326 **Exposure of cholangiocytes to *H. pylori* induces cellular migration, invasion and wound**
327 **closure**
328
329 Analysis in real time with a Boyden chamber-type apparatus revealed that exposure to *H. pylori*
330 at MOI of 10 to 50 *H. pylori* significantly stimulated migration of H69 cells from 24 to 96 hours
331 after starting the assay (Figure 3A; *P* values at representative times and MOIs). The effect was
332 not evident at MOI 100. A similar assay was undertaken using the CC-LP-1 cholangiocarcinoma
333 cell line but with at lower MOI. At MOI of 1, 10 and 50, *H. pylori* stimulated significantly more
334 migration of CC-LP-1 cells from 20 to 40 hours after starting the assay (Figure 3B). Concerning
335 invasion of extracellular matrix, both the CC-LP-1 and H69 cells migrated and invaded the
336 Matrigel layer in the UC of the CIM plate at significantly higher rates than did the control cells,
337 with significant differences evident from 48 to 96 hours (Figure 3, C,D). In addition, scratch
338 assays revealed two-dimensional migration of H69 cells over 24 hours. Wound closure by H69
339 cells increased significantly to 19.47% at MOI of 10 ($P \leq 0.05$) although an effect at MOI 100
340 was not apparent in comparison with the control group (Figure 4).
341
342 ***H. pylori* induces anchorage-independent colony formation**
343
344 As a prospective biomarker of malignant transformation of the *Helicobacter*-infected
345 cholangiocytes, anchorage independent colony formation by the cells was determined in a
346 medium of soft agar. Following maintenance of the cultures for up to 28 days, counts of the
347 numbers of colonies was revealed that a MOI of 10 *H. pylori* had induced a significant increase
348 colony numbers of the H69 cells (Figure 5A, B). Significant differences from the control group
349 were not seen at MOI 50 or 100. The size of colonies also increased in all groups exposed to *H.*
350 *pylori* although this was statistically significant only at the MOI of 50 (Figure S2; $P \leq 0.05$). By
351 contrast to *H. pylori*, exposure of H69 cells to *H. bilis*, a microbe that naturally resides in the
352 biliary tract and intestines [40, 64], decreased the number of colony formation in soft agar
353 (Figure 5C). The neutral or even inhibitory effect of *H. bilis* on H69 was mirrored by the lack of
354 cellular proliferation by H69 cells when monitored in real-time over 72 hours days at MOI of 0,
355 10, 50, and 100 *H. bilis* (Figure S3).
356
357 **Discussion**
358
359 Numerous species of *Helicobacter* have been described [65] while *H. pylori* was the first
360 prokaryote confirmed to cause gastric disease, including peptic ulcer, gastric mucosa-associated
361 tissue lymphoma, and adenocarcinoma [38, 66-69]. Bacilli of *H. pylori* occur in the stomach in at
362 least half of the human population. Transmission is from mother to child and by other routes.
363 The human-*H. pylori* association may be beneficial in early life, including contributions to a
364 healthy microbiome and reduced early-onset asthma [70, 71]. Strains of *H. pylori* have been
365 characterized at the molecular level, and classified as either CagA (cytotoxin-associated gene A)
366 -positive or -negative. CagA, the major virulence factor of *H. pylori*, is a ~140 kDa protein
367 encoded on the Cag pathogenicity island, PAI. Cag PAI also encodes a type 4 secretion channel

368 through which the virulence factor is introduced into the host cell [29]. CagA locates to the cell
369 membrane, where it is phosphorylated by the Src kinases. Downstream of these modifications,
370 the activated CagA orchestrates changes in morphology of the epithelial cell, which loses cell
371 polarity and becomes motile, transforming in appearance to the hallmark 'hummingbird-like'
372 phenotype [72-74].
373
374 The CagA oncoprotein is noted for its variation at the SHP2 binding site and, based on the
375 sequence variation, is subclassified into two main types, East-Asian and Western CagA. East-
376 Asian CagA shows stronger SHP2 binding and greater biological activity than the Western
377 genotype. In East Asia, the circulation of *H. pylori* strains encoding active forms of CagA may
378 underlie the elevated incidence of gastric adenocarcinoma [29]. In addition to the well-known
379 association with gastric cancer, *H. pylori* has been associated with hepatobiliary disease [4, 5,
380 75]. Related species of *Helicobacter*, *H. hepaticus* and *H. bilis*, also associate with hepatobiliary
381 disease [75-77]. Infection with the fish-borne liver flukes, *Opisthorchis viverrini* and *Clonorchis*
382 *sinensis*, as well as the infection with *H. pylori* are all classified as Group 1 carcinogens by the
383 International Agency for Research on Cancer [6]. Opisthorchiasis is a major risk factor for
384 cholangiocarcinoma in northeastern Thailand and Laos [6-9]. In addition to gastric disease,
385 infection with species of *Helicobacter* causes hepatobiliary tract diseases that can resemble
386 opisthorchiasis [5, 8, 9, 11, 12]. Liver fluke infection can induce lesions in biliary system
387 including cholangitis, biliary hyperplasia and metaplasia, periductal fibrosis and CCA. These
388 lesions derive not only from liver fluke infection but perhaps are in part the consequence of
389 hepatobiliary tract infection with *H. pylori*. *Helicobacter* may transit from the stomach to the
390 duodenum and enter the biliary tree through the duodenal papilla and ampulla of Vater [26, 78],
391 and indeed may be vectored there by the liver fluke, *O. viverrini* [1-3]. *H. pylori*-specific DNA
392 sequences have been detected in CCA tumors and also from lesions diagnosed as
393 cholecystitis/cholelithiasis in regions endemic for opisthorchiasis [5, 11]. Furthermore,
394 serological findings have implicated infection with *H. pylori* as a risk for CCA in Thailand [12].
395
396 Here, we investigated interactions among a human cholangiocyte cell line, H69, a CCA cell line
397 CC-LP-1, CagA^{+} *H. pylori*, and *H. bilis* bacilli. Infection of H69 with CagA^{+} *H. pylori* induced
398 EMT in dose-dependent manner, which was characterized by cell elongation and scattering
399 which, in turn, implicate increasing change in cell motility. This visible appearance of these
400 infected H69 cells resembled the hummingbird phenotype of gastric epithelial cells after
401 exposure *H. pylori* [28, 29, 79]. In the AGS cell line, delivery of CagA by the type IV secretion
402 mechanism from *H. pylori* subverts the normal signaling leading to actin-dependent
403 morphological rearrangement. The hitherto uniform polygonal shape becomes markedly
404 elongated with terminal needle-like projections [80].
405
406 AGS cells infected with *H. pylori* demonstrating the hummingbird phenotype also display early
407 transcriptional changes that reflect EMT [28]. H69 cells infected with *H. pylori* exhibited
408 upregulation of expression of Snail, Slug, vimentin, JAM1, and MMP7 in a dose-dependent
409 fashion, changes that strongly supported the EMT of this informative cholangiocyte cell line.
410 Likewise, Snail, an *E*-cadherin repressor, was markedly up-regulated, which indicated that this
411 factor may be a key driver of EMT in cholangiocytes. CD44 expression was up-regulated in
412 dose-dependent fashion, whereas CD24 decreased, showing a CD44^{+}/CD24$^{-/low}$ phenotype

during infection. *H. pylori* may not only induce EMT but also contribute to stemness and malignant transformation of the cholangiocyte [63, 81].

Realtime cell monitoring revealed that the H69 and CC-LP-1 cells migrated when exposed to *H. pylori*. Moreover, 10 bacilli of *H. pylori* per biliary cell stimulated cellular migration and invasion through a basement membrane matrix, a behavioral phenotype also characteristic of EMT. In addition, following exposure to *H. pylori*, H69 cells responded with an anchorage-independent cell growth in soft agar, a phenotype indicative of the escape from anoikis and characteristic of metastasis [82]. The numbers of colonies of H69 cells in soft agar significantly increased following exposure to *H. pylori* at MOI of 10. By contrast, monitoring contact-independent cell growth in soft agar and also growth responses by H69 cells as monitored and quantified using the RTCA approach, both the numbers of colonies of H69 in soft agar and cell growth during the RTCA assay both decreased. The responses indicated that CagA$^+$ *H. pylori*, but not *H. bilis*, displays the potential to induce neoplastic changes in cholangiocytes in like fashion to its carcinogenicity for the gastric epithelia.

The findings presented here notwithstanding, the report has some limitations. We utilized the ATCC 43504 CagA positive strain to investigate responses from the human cholangiocyte to *H. pylori*. However, repeat assays using other CagA positive strains such as P12 [83] could buttress the present findings and, as well, exclude strain-specific effects. Furthermore, inclusion of a CagA negative and/or *cag*PAI-dysfunctional strain such as SS1 would explore the specific contribution of CagA [84-86]. Second, induction of the hummingbird phenotype in gastric epithelial cells by the CagA+ *H. pylori* is dependent on the number and type of EPIYA phosphorylation site repeats [73, 87]. To confirm that Cag A+ *H. pylori* can also induce a hummingbird-like phenotype of the cholangiocyte, a demonstration that H69 cells can be infected by the *H. pylori*, and the *cag*PAI is functional during the infection, as established by detection of phosphorylated CagA, would be needed [88-90].

The present findings supported the hypothesis that opisthorchiasis and *H. pylori* together may hasten or even synergize the malignant transformation of cholangiocytes [2, 3, 91]. By contrast, co-infections of *Helicobacter* species including *H. pylori* and some other helminths have generally been associated with diminished risk of *H. pylori*-associated gastric carcinoma [92-94]. Notably, concurrent infection on mice with an intestinal nematode modulates inflammation, induces a Th2-polarizing cytokine phenotype with concomitant downmodulation of Th1 and the gastric immune responses, and reduces *Helicobacter*-induced gastric atrophy [95]. Nonetheless, given that CagA$^+$ *H. pylori* stimulated EMT in cholangiocytes and which, in turn, also suggests a role in the underlying fibrosis [96-98] and metastasis [99-101] of cholangiocarcinoma, an explanation for why infection with the liver fluke induces CCA might now be somewhat clearer – involvement by *H. pylori* and its virulence factors [102, 103].

Conclusions

Infection with CagA$^+$ *H. pylori* induced epithelial to mesenchymal transition in human cholangiocytes. Further investigation of the relationship between *O. viverrini* and *H. pylori* within the infected biliary tract is warranted. Studies on tumorigenicity of the *H. pylori*-transformed H69 cells in immune-suppressed mice would likely be informative.

Abbreviations

CCA, cholangiocarcinoma; EMT, epithelial to mesenchymal transition; CagA, cytotoxin-associated gene A; ZEB1, zinc finger E-box-binding homeobox 1; JAM1, junctional adhesion molecule 1; MMP7, matrix metalloprotease 7; CD24, cluster of differentiation marker 24; CD44, cluster of differentiation marker 44; MOI, multiplicity of infection; RTCA, real time cell analysis; CI, cell index; UC, upper chamber (of Boyden chamber); LC, lower chamber.

Competing Financial Interests

The authors declare there were no competing financial interests.

Acknowledgments

P.T. acknowledges support as a PhD research scholar from the Thailand Research Fund under the Royal Golden Jubilee scholars program (grant number PHD/0013/2555); B.S. acknowledges support from Thailand Research Fund Senior Research Scholar. This work was supported by the National Health Security Office, Thailand, the Higher Education Research Promotion and National Research University Project of Thailand, Office of the Higher Education Commission, through the Health Cluster (SHeP-GMS), the Faculty of Medicine, Khon Kaen University, Thailand (award number I56110), and the Thailand Research Fund under the TRF Senior Research Scholar (RTA 5680006); the National Research Council of Thailand. The National Institute of Allergy and Infectious Diseases (NIAID), Tropical Medicine Research Center award number P50AI098639, The National Cancer Institute (NCI), award number R01CA164719, and the United States Army Medical Research and Materiel Command (USAMRMC), contract number W81XWH-12-C-0267 also provided support. The content is solely the responsibility of the authors and does not necessarily represent the official views of the funders including USAMRMC, NIAID, NCI or the NIH. This manuscript has been released as a pre-print at *bioRxiv* [Thanaphongdecha et al [104]].

Author contributions

P.T., S.S., C.P., Y.C., J.F., B.S. and P.J.B. conceived and designed the study. P.T., S.K., V.M., W.I. performed the experiments. P.T., W.I., B.S. and PJB analyzed and interpreted the findings. P.T., B.S., W.I., S.S., and PJB wrote the manuscript. All authors read and approved the final version of the paper.

505 **Figure legends**

506 **Figure 1. Exposure to CagA$^+$ *Helicobacter pylori* ATCC 43504 induced morphological**
507 **alteration in cholangiocytes including cell elongation, indicative of epidermal to**
508 **mesenchymal transition**. Panels A-C: photomicrographs documenting cell morphology of H69
509 cells exposed to increasing numbers of *H. pylori* at 0, 10, and 100 bacilli per cholangiocyte,
510 respectively (left to right). The appearance of cells changed from an epithelial to a mesenchymal
511 phenotype as evidenced by the loss of cell-cell contact, an elongated and spindle-shaped
512 morphology, along with growth as individual cells by 24 hours following *H. pylori* infection in a
513 dose-dependent manner. Scale bars, 5 μm (right), 20× magnification. The length-to-width ratio
514 of single, isolated single cells were documented to determine cellular elongation and scattering
515 (D, E). The number of elongated cells increased in a dose-dependent fashion in response to
516 infection by *H. pylori* (F). By contrast, the number of isolated individual H69 cells, indicative of
517 cell scattering, was also significantly increased in dose-dependent fashion (G). Data are
518 presented as the mean ± standard error of three biological replicates. Means were compared
519 using one-way ANOVA. Asterisks indicate levels of statistical significance of experimental
520 compared to control groups at 24 hours; *, $P \leq 0.05$; **, $P \leq 0.01$; ***, $P \leq 0.001$; ****, $P \leq$
521 0.0001.
522
523 **Figure 2. Differential transcript fold change of EMT-related and cancer stem cell marker**
524 **genes after exposure to *Helicobacter pylori*.** Messenger RNA expression of six EMT-related
525 genes and two cancer stem cell markers were determined after 24 hours of infection. Expression
526 of Snail, Slug, vimentin, JAM1, MMP7, and CD44 increased in a dose fashion whereas CD24
527 transcription decreased. Expression of the regulatory transcriptional factor, Snail was notably up-
528 regulated by 6.27±1.02-, 9.05±1.28- and 12.25±0.78-fold at MOI 10, 50, and 100, respectively.
529 MMP7 expression was markedly up-regulated by 3.3 to 5.3 fold at each MOI. Expression of each
530 of Slug, ZEB1, vimentin, and JAM1 was up-regulated in a dose dependent fashion.
531 Transcription of the cancer stem cell marker CD44 was significantly up-regulated by 2.02±0.88
532 fold at MOI 50 and by 3.75±0.60 fold at MO of 100 whereas no significant change was seen with
533 CD24. Three biological replicates were carried out. The qPCR findings were normalized to the
534 expression levels of GAPDH in each sample, with the mean ± S.D. values shown for the seven
535 genes at each of MOI of 10, 50 and 100, and compared using a two-way ANOVA multiple
536 comparison with a 95% confidence interval of difference.
537
538 **Figure 3. Exposing cholangiocytes to *H. pylori* induced migration and invasion through**
539 **extracellular matrix.** H69 cholangiocytes infected with *H. pylori* migrated through Matrigel, as
540 monitored in real time over 100 hours using CIM plates fitted to a xCELLigence DP system. Cell
541 migration and invasion were monitored for 100 hours with chemo-attractant in the lower
542 chamber of CIM plate. H69 cells infected with MOI 10 exhibited the highest cell migration rate
543 followed by MOI 50 whereas MOI 100 attenuated cell migration to a level comparable with non-
544 infected control (A). Similarly, the cholangiocarcinoma cell line CC-LP-1 showed the highest
545 cell migration rate when stimulated with MOI 10 followed by MOI 50. Moreover, CC-LP-1 cells
546 significantly migrated faster even with at MOI of 1 (B). Invasion of the Matrigel extracellular
547 matrix compared between MOI 10 and non-infected cells; invasion rates for CC-LP-1 and H69
548 cells significantly increased following exposure to *H. pylori* (C,D).
549

550 **Figure 4. Wound healing in a two-dimensional *in vitro* assay revealed cell migration of H69**
551 **cholangiocytes infected with *H. pylori*.** Wound closure was significantly increased to 19.47% at
552 MOI 10 of *H. pylori* ($P \leq 0.05$) by one-way ANOVA. An increase in wound closure was not
553 apparent at MOI 100; 11.09% vs control, 14.47%. Micrographs at 0 (left) and 26 (right) hours;
554 5× magnification.
555
556 **Figure 5. Anchorage-independent cell growth in soft agar revealed cellular transformation**
557 **of cholangiocytes by *H. pylori*.** Representative micrographs revealing the appearance of
558 colonies of H69 cholangiocytes at 30 days following exposure to *H. pylori* and to *H. bilis*, as
559 indicated (A). At MOI of 10, the number of H69 cell colonies increased significantly ($P \leq 0.01$),
560 whereas not at MOI of 50; by contrast, there was a significant decrease in colony numbers at
561 MOI of 100, when compared with the non-infected control cells (B). Exposure of H69 cells to *H.*
562 *bilis* resulted in markedly reduced numbers of colonies, in a dose-dependent fashion (C; $P \leq$
563 0.001), indicating an inhibitory effect of *H. bilis* toward anchorage-independent cell growth
564 and/or cellular transformation of human cholangiocytes (C). Three biological replicates were
565 performed.
566
567
568 **Supporting information**
569
570 **Figure S1. TGF-β promoted nodule formation.** TGF-β, an EMT-stimulant, induced nodule
571 formation of H69 cholangiocytes. Cells were cultured in the presence of 5 ng/ml TGF-β in
572 serum- and hormone-free medium for 24 hours. Micrographs at 0 (left) and 24 (right) hours;
573 5×magnification.

574 **Figure S2. Size of colonies of cholangiocytes in soft agar.** Colonies with a diameter ≥ 50 µm
575 were counted and the diameter measured; mean values were 77.63, 91.62, 95.25 and 81.46 µm
576 diameter at MOI of 0, 10, 50, and 100, respectively.
577
578 **Figure S3. Growth of *Helicobacter bilis*-infected cholangiocytes as determined by the**
579 **xCELLigence approach.** H69 cells were exposed to increasing numbers of *H. bilis* (ATCC
580 43879) at MOI of 0, 10, 50, and 100. Cell growth was inhibited when compared to the uninfected
581 cells, at all MOIs. Assay was performed in E-plates in minimal (serum-depleted) medium [36].
582
583
584
585
586
587
588
589
590
591
592
593

Table S1. Nucleotide sequences of primers specific for human EMT-associated and cancer stem cell maker genes.

Gene	GenBank accession	Primer sequence, 5'-3'	Amplicon size (bp)
CD24	NM_013230.3	Forward CACCCAGCATCCTGCTAGAC	259
		Reverse GAGACCACGAAGAGACTGGC	
CD44	NM_00610.3	Forward GGGAGTCAAGAAGGTGGAGC	237
		Reverse CTGAGACTTGCTGGCCTCTC	
F11r/Jam1	NM_016946.5	Forward GTGCCTACTCGGGCTTTTCT	201
		Reverse GAGCTTGACCTTGACCTCCC	
Gapdh	NM_002046.5	Forward CCCATGTTCGTCATGGGTGT	366
		Reverse TTCTAGACGGCAGGTCAGGT	
MMP7	NM_002423.5	Forward GGAGCTCATGGGGACTCCTA	172
		Reverse GGCCAAGTTCATGAGTTGCAG	
Snai1	NM_005985.3	Forward AGCTCTCTGAGGCCAAGGAT	325
		Reverse GACATTCGGGAGAAGGTCCG	
Vimentin	NM_003380.5	Forward GCAGGAGGCAGAAGAATGGT	216
		Reverse GCAGCTTCAACGGCAAAGTT	
Zeb1	NM_001128128.2	Forward CGCAGTCTGGGTGTAATCGT	477
		Reverse CCATGCCCTGAGGAGAACTG	

622 **References**
623

624 1. Deenonpoe, R., et al., *The carcinogenic liver fluke Opisthorchis viverrini is a reservoir*
625 *for species of Helicobacter.* Asian Pac J Cancer Prev, 2015. **16**(5): p. 1751-8.
626 2. Deenonpoe, R., et al., *Elevated prevalence of Helicobacter species and virulence factors*
627 *in opisthorchiasis and associated hepatobiliary disease.* Sci Rep, 2017. **7**: p. 42744.
628 3. Sripa, B., R. Deenonpoe, and P.J. Brindley, *Co-infections with liver fluke and*
629 *Helicobacter species: A paradigm change in pathogenesis of opisthorchiasis and*
630 *cholangiocarcinoma?* Parasitol Int, 2017. **66**(4): p. 383-389.
631 4. Boonyanugomol, W., et al., *Effects of Helicobacter pylori gamma-*
632 *glutamyltranspeptidase on apoptosis and inflammation in human biliary cells.* Dig Dis
633 Sci, 2012. **57**(10): p. 2615-24.
634 5. Boonyanugomol, W., et al., *Helicobacter pylori in Thai patients with*
635 *cholangiocarcinoma and its association with biliary inflammation and proliferation.*
636 HPB (Oxford), 2012. **14**(3): p. 177-84.
637 6. Humans, I.W.G.o.t.E.o.C.R.t., *Biological agents. Volume 100 B. A review of human*
638 *carcinogens.* IARC Monogr Eval Carcinog Risks Hum, 2012. **100**(Pt B): p. 1-441.
639 7. Sungkasubun, P., et al., *Ultrasound screening for cholangiocarcinoma could detect*
640 *premalignant lesions and early-stage diseases with survival benefits: a population-based*
641 *prospective study of 4,225 subjects in an endemic area.* BMC Cancer, 2016. **16**: p. 346.
642 8. Khuntikeo, N., et al., *A Comprehensive Public Health Conceptual Framework and*
643 *Strategy to Effectively Combat Cholangiocarcinoma in Thailand.* PLoS Negl Trop Dis,
644 2016. **10**(1): p. e0004293.
645 9. Aye Soukhathammavong, P., et al., *Subtle to severe hepatobiliary morbidity in*
646 *Opisthorchis viverrini endemic settings in southern Laos.* Acta Trop, 2015. **141**(Pt B): p.
647 303-9.
648 10. Segura-Lopez, F.K., A. Guitron-Cantu, and J. Torres, *Association between Helicobacter*
649 *spp. infections and hepatobiliary malignancies: a review.* World J Gastroenterol, 2015.
650 **21**(5): p. 1414-23.
651 11. Boonyanugomol, W., et al., *Molecular analysis of Helicobacter pylori virulent-*
652 *associated genes in hepatobiliary patients.* HPB (Oxford), 2012. **14**(11): p. 754-63.
653 12. Pisani, P., et al., *Cross-reactivity between immune responses to Helicobacter bilis and*
654 *Helicobacter pylori in a population in Thailand at high risk of developing*
655 *cholangiocarcinoma.* Clin Vaccine Immunol, 2008. **15**(9): p. 1363-8.
656 13. Lvova, M.N., et al., *Comparative histopathology of Opisthorchis felineus and*
657 *Opisthorchis viverrini in a hamster model: an implication of high pathogenicity of the*
658 *European liver fluke.* Parasitol Int, 2012. **61**(1): p. 167-72.
659 14. Mairiang, E., et al., *Ultrasonography assessment of hepatobiliary abnormalities in 3359*
660 *subjects with Opisthorchis viverrini infection in endemic areas of Thailand.* Parasitol Int,
661 2012. **61**(1): p. 208-11.
662 15. Kao, C.Y., B.S. Sheu, and J.J. Wu, *Helicobacter pylori infection: An overview of*
663 *bacterial virulence factors and pathogenesis.* Biomed J, 2016. **39**(1): p. 14-23.
664 16. Cid, T.P., et al., *Pathogenesis of Helicobacter pylori infection.* Helicobacter, 2013. **18**
665 **Suppl 1**: p. 12-7.
666 17. Hatakeyama, M., *Helicobacter pylori CagA and gastric cancer: a paradigm for hit-and-*
667 *run carcinogenesis.* Cell Host Microbe, 2014. **15**(3): p. 306-16.

668 18. Cover, T.L., D.B. Lacy, and M.D. Ohi, *The Helicobacter pylori Cag Type IV Secretion*
669 *System.* Trends Microbiol, 2020. **28**(8): p. 682-695.
670 19. Fox, J.G., et al., *Hepatic Helicobacter species identified in bile and gallbladder tissue*
671 *from Chileans with chronic cholecystitis.* Gastroenterology, 1998. **114**(4): p. 755-63.
672 20. Pellicano, R., et al., *Helicobacter species sequences in liver samples from patients with*
673 *and without hepatocellular carcinoma.* World J Gastroenterol, 2004. **10**(4): p. 598-601.
674 21. Nilsson, H.O., et al., *Helicobacter species identified in liver from patients with*
675 *cholangiocarcinoma and hepatocellular carcinoma.* Gastroenterology, 2001. **120**(1): p.
676 323-4.
677 22. Huang, Y., et al., *Identification of helicobacter species in human liver samples from*
678 *patients with primary hepatocellular carcinoma.* J Clin Pathol, 2004. **57**(12): p. 1273-7.
679 23. Knorr, J., et al., *Classification of Helicobacter pylori Virulence Factors: Is CagA a Toxin*
680 *or Not?* Trends Microbiol, 2019. **27**(9): p. 731-738.
681 24. Boonyanugomol, W., et al., *Role of cagA-positive Helicobacter pylori on cell*
682 *proliferation, apoptosis, and inflammation in biliary cells.* Dig Dis Sci, 2011. **56**(6): p.
683 1682-92.
684 25. Plieskatt, J.L., et al., *Infection with the carcinogenic liver fluke Opisthorchis viverrini*
685 *modifies intestinal and biliary microbiome.* FASEB J, 2013. **27**(11): p. 4572-84.
686 26. Boonyanugomol, W., et al., *Helicobacter pylori cag pathogenicity island (cagPAI)*
687 *involved in bacterial internalization and IL-8 induced responses via NOD1- and MyD88-*
688 *dependent mechanisms in human biliary epithelial cells.* PLoS One, 2013. **8**(10): p.
689 e77358.
690 27. Fung, C., et al., *High-resolution mapping reveals that microniches in the gastric glands*
691 *control Helicobacter pylori colonization of the stomach.* PLoS Biol, 2019. **17**(5): p.
692 e3000231.
693 28. Lamouille, S., J. Xu, and R. Derynck, *Molecular mechanisms of epithelial-mesenchymal*
694 *transition.* Nat Rev Mol Cell Biol, 2014. **15**(3): p. 178-96.
695 29. Hatakeyama, M., *Oncogenic mechanisms of the Helicobacter pylori CagA protein.* Nat
696 Rev Cancer, 2004. **4**(9): p. 688-94.
697 30. Fox, J.G., *Helicobacter bilis: bacterial provocateur orchestrates host immune responses*
698 *to commensal flora in a model of inflammatory bowel disease.* Gut, 2007. **56**(7): p. 898-
699 900.
700 31. Grubman, S.A., et al., *Regulation of intracellular pH by immortalized human*
701 *intrahepatic biliary epithelial cell lines.* Am J Physiol, 1994. **266**(6 Pt 1): p. G1060-70.
702 32. Park, J., G.J. Gores, and T. Patel, *Lipopolysaccharide induces cholangiocyte proliferation*
703 *via an interleukin-6-mediated activation of p44/p42 mitogen-activated protein kinase.*
704 Hepatology, 1999. **29**(4): p. 1037-43.
705 33. Bairoch, A., *The Cellosaurus, a Cell-Line Knowledge Resource.* J Biomol Tech, 2018.
706 **29**(2): p. 25-38.
707 34. Shimizu, Y., et al., *Two new human cholangiocarcinoma cell lines and their cytogenetics*
708 *and responses to growth factors, hormones, cytokines or immunologic effector cells.* Int J
709 Cancer, 1992. **52**(2): p. 252-60.
710 35. Han, C., et al., *PPARgamma ligands inhibit cholangiocarcinoma cell growth through*
711 *p53-dependent GADD45 and p21 pathway.* Hepatology, 2003. **38**(1): p. 167-77.

712 36. Smout, M.J., et al., *Carcinogenic Parasite Secretes Growth Factor That Accelerates*
713 *Wound Healing and Potentially Promotes Neoplasia.* PLoS Pathog, 2015. **11**(10): p.
714 e1005209.
715 37. Arunsan, P., et al., *Programmed knockout mutation of liver fluke granulin attenuates*
716 *virulence of infection-induced hepatobiliary morbidity.* Elife, 2019. **8**.
717 38. Marshall, B.J. and J.R. Warren, *Unidentified curved bacilli in the stomach of patients*
718 *with gastritis and peptic ulceration.* Lancet, 1984. **1**(8390): p. 1311-5.
719 39. Dewhirst, F.E., et al., *'Flexispira rappini' strains represent at least 10 Helicobacter taxa.*
720 Int J Syst Evol Microbiol, 2000. **50 Pt 5**: p. 1781-1787.
721 40. Fox, J.G., et al., *Helicobacter bilis sp. nov., a novel Helicobacter species isolated from*
722 *bile, livers, and intestines of aged, inbred mice.* J Clin Microbiol, 1995. **33**(2): p. 445-54.
723 41. Hachem, C.Y., et al., *Comparison of agar based media for primary isolation of*
724 *Helicobacter pylori.* J Clin Pathol, 1995. **48**(8): p. 714-6.
725 42. Jung, S.W., et al., *Mechanism of antibacterial activity of liposomal linolenic acid against*
726 *Helicobacter pylori.* PLoS One, 2015. **10**(3): p. e0116519.
727 43. Lin, S.N., et al., *Helicobacter pylori heat-shock protein 60 induces production of the pro-*
728 *inflammatory cytokine IL8 in monocytic cells.* J Med Microbiol, 2005. **54**(Pt 3): p. 225-
729 233.
730 44. Pan, H., et al., *A comparison of conventional methods for the quantification of bacterial*
731 *cells after exposure to metal oxide nanoparticles.* BMC Microbiol, 2014. **14**: p. 222.
732 45. Masuda, M., et al., *Tumor suppressor in lung cancer (TSLC)1 suppresses epithelial cell*
733 *scattering and tubulogenesis.* J Biol Chem, 2005. **280**(51): p. 42164-71.
734 46. Bourzac, K.M., L.A. Satkamp, and K. Guillemin, *The Helicobacter pylori cag*
735 *pathogenicity island protein CagN is a bacterial membrane-associated protein that is*
736 *processed at its C terminus.* Infect Immun, 2006. **74**(5): p. 2537-43.
737 47. Nagy, T.A., et al., *Helicobacter pylori regulates cellular migration and apoptosis by*
738 *activation of phosphatidylinositol 3-kinase signaling.* J Infect Dis, 2009. **199**(5): p. 641-
739 51.
740 48. Bindschadler, M. and J.L. McGrath, *Sheet migration by wounded monolayers as an*
741 *emergent property of single-cell dynamics.* J Cell Sci, 2007. **120**(Pt 5): p. 876-84.
742 49. Liang, C.C., A.Y. Park, and J.L. Guan, *In vitro scratch assay: a convenient and*
743 *inexpensive method for analysis of cell migration in vitro.* Nat Protoc, 2007. **2**(2): p. 329-
744 33.
745 50. Livak, K.J. and T.D. Schmittgen, *Analysis of relative gene expression data using real-*
746 *time quantitative PCR and the 2(-Delta Delta C(T)) Method.* Methods, 2001. **25**(4): p.
747 402-8.
748 51. Ye, J., et al., *Primer-BLAST: a tool to design target-specific primers for polymerase*
749 *chain reaction.* BMC Bioinformatics, 2012. **13**: p. 134.
750 52. Arunsan, P., et al., *Liver fluke granulin promotes extracellular vesicle-mediated crosstalk*
751 *and cellular microenvironment conducive to cholangiocarcinoma.* Neoplasia, 2020.
752 **22**(5): p. 203-216.
753 53. Ke, N., et al., *The xCELLigence system for real-time and label-free monitoring of cell*
754 *viability.* Methods Mol Biol, 2011. **740**: p. 33-43.
755 54. Dowling, C.M., C. Herranz Ors, and P.A. Kiely, *Using real-time impedance-based assays*
756 *to monitor the effects of fibroblast-derived media on the adhesion, proliferation,*
757 *migration and invasion of colon cancer cells.* Biosci Rep, 2014. **34**(4).

758 55. Matchimakul, P., et al., *Apoptosis of cholangiocytes modulated by thioredoxin of*
759 *carcinogenic liver fluke.* Int J Biochem Cell Biol, 2015. **65**: p. 72-80.
760 56. Rinaldi, G., et al., *Cytometric analysis, genetic manipulation and antibiotic selection of*
761 *the snail embryonic cell line Bge from Biomphalaria glabrata, the intermediate host of*
762 *Schistosoma mansoni.* Int J Parasitol, 2015. **45**(8): p. 527-35.
763 57. Solly, K., et al., *Application of real-time cell electronic sensing (RT-CES) technology to*
764 *cell-based assays.* Assay Drug Dev Technol, 2004. **2**(4): p. 363-72.
765 58. Xie, H., et al., *Novel functions and targets of miR-944 in human cervical cancer cells.* Int
766 J Cancer, 2015. **136**(5): p. E230-41.
767 59. Horibata, S., et al., *Utilization of the Soft Agar Colony Formation Assay to Identify*
768 *Inhibitors of Tumorigenicity in Breast Cancer Cells.* J Vis Exp, 2015(99): p. e52727.
769 60. Zeisberg, M. and E.G. Neilson, *Biomarkers for epithelial-mesenchymal transitions.* J Clin
770 Invest, 2009. **119**(6): p. 1429-37.
771 61. Nieto, M.A., *The snail superfamily of zinc-finger transcription factors.* Nat Rev Mol Cell
772 Biol, 2002. **3**(3): p. 155-66.
773 62. Boulay, J.L., C. Dennefeld, and A. Alberga, *The Drosophila developmental gene snail*
774 *encodes a protein with nucleic acid binding fingers.* Nature, 1987. **330**(6146): p. 395-8.
775 63. Nguyen, P.H., et al., *Characterization of Biomarkers of Tumorigenic and Chemoresistant*
776 *Cancer Stem Cells in Human Gastric Carcinoma.* Clin Cancer Res, 2017. **23**(6): p. 1586-
777 1597.
778 64. Shomer, N.H., et al., *Helicobacter bilis-induced inflammatory bowel disease in scid mice*
779 *with defined flora.* Infect Immun, 1997. **65**(11): p. 4858-64.
780 65. Flahou, B., et al., *The Other Helicobacters.* Helicobacter, 2015. **20 Suppl 1**: p. 62-7.
781 66. Cover, T.L., *Helicobacter pylori Diversity and Gastric Cancer Risk.* MBio, 2016. **7**(1): p.
782 e01869-15.
783 67. Marshall, B.J., *The pathogenesis of non-ulcer dyspepsia.* Med J Aust, 1985. **143**(7): p.
784 319.
785 68. Gaynor, E.C. and C.M. Szymanski, *The 30th anniversary of Campylobacter,*
786 *Helicobacter, and Related Organisms workshops-what have we learned in three*
787 *decades?* Front Cell Infect Microbiol, 2012. **2**: p. 20.
788 69. Sheh, A. and J.G. Fox, *The role of the gastrointestinal microbiome in Helicobacter pylori*
789 *pathogenesis.* Gut Microbes, 2013. **4**(6): p. 505-31.
790 70. Kienesberger, S., et al., *Gastric Helicobacter pylori Infection Affects Local and Distant*
791 *Microbial Populations and Host Responses.* Cell Rep, 2016. **14**(6): p. 1395-407.
792 71. Cover, T.L. and M.J. Blaser, *Helicobacter pylori in health and disease.* Gastroenterology,
793 2009. **136**(6): p. 1863-73.
794 72. Saadat, I., et al., *Helicobacter pylori CagA targets PAR1/MARK kinase to disrupt*
795 *epithelial cell polarity.* Nature, 2007. **447**(7142): p. 330-3.
796 73. Hatakeyama, M. and H. Higashi, *Helicobacter pylori CagA: a new paradigm for*
797 *bacterial carcinogenesis.* Cancer Sci, 2005. **96**(12): p. 835-43.
798 74. Yamaoka, Y., *Mechanisms of disease: Helicobacter pylori virulence factors.* Nat Rev
799 Gastroenterol Hepatol, 2010. **7**(11): p. 629-41.
800 75. Murphy, G., et al., *Association of seropositivity to Helicobacter species and biliary tract*
801 *cancer in the ATBC study.* Hepatology, 2014. **60**(6): p. 1963-71.
802 76. Mateos-Munoz, B., et al., *Enterohepatic Helicobacter other than Helicobacter pylori.*
803 Rev Esp Enferm Dig, 2013. **105**(8): p. 477-84.

804 77. Zhou, D., et al., *Infections of Helicobacter spp. in the biliary system are associated with*
805 *biliary tract cancer: a meta-analysis.* Eur J Gastroenterol Hepatol, 2013. **25**(4): p. 447-
806 54.
807 78. Pellicano, R., et al., *Helicobacter species and liver diseases: association or causation?*
808 Lancet Infect Dis, 2008. **8**(4): p. 254-60.
809 79. Wroblewski, L.E., R.M. Peek, Jr., and K.T. Wilson, *Helicobacter pylori and gastric*
810 *cancer: factors that modulate disease risk.* Clin Microbiol Rev, 2010. **23**(4): p. 713-39.
811 80. Segal, E.D., et al., *Altered states: involvement of phosphorylated CagA in the induction of*
812 *host cellular growth changes by Helicobacter pylori.* Proc Natl Acad Sci U S A, 1999.
813 **96**(25): p. 14559-64.
814 81. Klonisch, T., et al., *Cancer stem cell markers in common cancers - therapeutic*
815 *implications.* Trends Mol Med, 2008. **14**(10): p. 450-60.
816 82. Simpson, C.D., K. Anyiwe, and A.D. Schimmer, *Anoikis resistance and tumor*
817 *metastasis.* Cancer Lett, 2008. **272**(2): p. 177-85.
818 83. Fischer, W., et al., *Strain-specific genes of Helicobacter pylori: genome evolution driven*
819 *by a novel type IV secretion system and genomic island transfer.* Nucleic Acids Res,
820 2010. **38**(18): p. 6089-101.
821 84. Lee, A., et al., *A standardized mouse model of Helicobacter pylori infection: introducing*
822 *the Sydney strain.* Gastroenterology, 1997. **112**(4): p. 1386-97.
823 85. Nolan, K.J., et al., *In vivo behavior of a Helicobacter pylori SS1 nixA mutant with*
824 *reduced urease activity.* Infect Immun, 2002. **70**(2): p. 685-91.
825 86. Kundu, P., et al., *Cag pathogenicity island-independent up-regulation of matrix*
826 *metalloproteinases-9 and -2 secretion and expression in mice by Helicobacter pylori*
827 *infection.* J Biol Chem, 2006. **281**(45): p. 34651-62.
828 87. Higashi, H., et al., *EPIYA motif is a membrane-targeting signal of Helicobacter pylori*
829 *virulence factor CagA in mammalian cells.* J Biol Chem, 2005. **280**(24): p. 23130-7.
830 88. Ren, S., et al., *Structural basis and functional consequence of Helicobacter pylori CagA*
831 *multimerization in cells.* J Biol Chem, 2006. **281**(43): p. 32344-52.
832 89. Backert, S., N. Tegtmeyer, and W. Fischer, *Composition, structure and function of the*
833 *Helicobacter pylori cag pathogenicity island encoded type IV secretion system.* Future
834 Microbiol, 2015. **10**(6): p. 955-65.
835 90. Tohidpour, A., *CagA-mediated pathogenesis of Helicobacter pylori.* Microb Pathog,
836 2016. **93**: p. 44-55.
837 91. Itthitaetrakool, U., et al., *Chronic Opisthorchis viverrini Infection Changes the Liver*
838 *Microbiome and Promotes Helicobacter Growth.* PLoS One, 2016. **11**(11): p. e0165798.
839 92. Holcombe, C., *Helicobacter pylori: the African enigma.* Gut, 1992. **33**(4): p. 429-31.
840 93. Du, Y., et al., *Helicobacter pylori and Schistosoma japonicum co-infection in a Chinese*
841 *population: helminth infection alters humoral responses to H. pylori and serum*
842 *pepsinogen I/II ratio.* Microbes Infect, 2006. **8**(1): p. 52-60.
843 94. Whary, M.T., et al., *Intestinal helminthiasis in Colombian children promotes a Th2*
844 *response to Helicobacter pylori: possible implications for gastric carcinogenesis.* Cancer
845 Epidemiol Biomarkers Prev, 2005. **14**(6): p. 1464-9.
846 95. Fox, J.G., et al., *Concurrent enteric helminth infection modulates inflammation and*
847 *gastric immune responses and reduces helicobacter-induced gastric atrophy.* Nat Med,
848 2000. **6**(5): p. 536-42.

849 96. Fragiadaki, M. and R.M. Mason, *Epithelial-mesenchymal transition in renal fibrosis -*
850 *evidence for and against.* Int J Exp Pathol, 2011. **92**(3): p. 143-50.
851 97. Rout-Pitt, N., et al., *Epithelial mesenchymal transition (EMT): a universal process in*
852 *lung diseases with implications for cystic fibrosis pathophysiology.* Respir Res, 2018.
853 **19**(1): p. 136.
854 98. Stone, R.C., et al., *Epithelial-mesenchymal transition in tissue repair and fibrosis.* Cell
855 Tissue Res, 2016. **365**(3): p. 495-506.
856 99. Kalluri, R. and R.A. Weinberg, *The basics of epithelial-mesenchymal transition.* J Clin
857 Invest, 2009. **119**(6): p. 1420-8.
858 100. Li, L. and W. Li, *Epithelial-mesenchymal transition in human cancer: comprehensive*
859 *reprogramming of metabolism, epigenetics, and differentiation.* Pharmacol Ther, 2015.
860 **150**: p. 33-46.
861 101. Sciacovelli, M. and C. Frezza, *Metabolic reprogramming and epithelial-to-mesenchymal*
862 *transition in cancer.* FEBS J, 2017. **284**(19): p. 3132-3144.
863 102. Brindley, P.J., J.M. da Costa, and B. Sripa, *Why does infection with some helminths cause*
864 *cancer?* Trends Cancer, 2015. **1**(3): p. 174-182.
865 103. Brindley, P.J. and A. Loukas, *Helminth infection-induced malignancy.* PLoS Pathog,
866 2017. **13**(7): p. e1006393.
867 104. Thanaphongdecha, P.K., S.E., Ittiprasrt, W., Mann, V.H., Chamgramol, Y., Pairojkul, C.,
868 Fox, J.G., Suttiprapa, S., Sripa, B., Brindley, P.J. , *Infection with CagA+ Helicobacter*
869 *pylori induces epithelial to mesenchymal transition in human cholangiocytes.* bioRxiv,
870 2020.
871

Figure 1

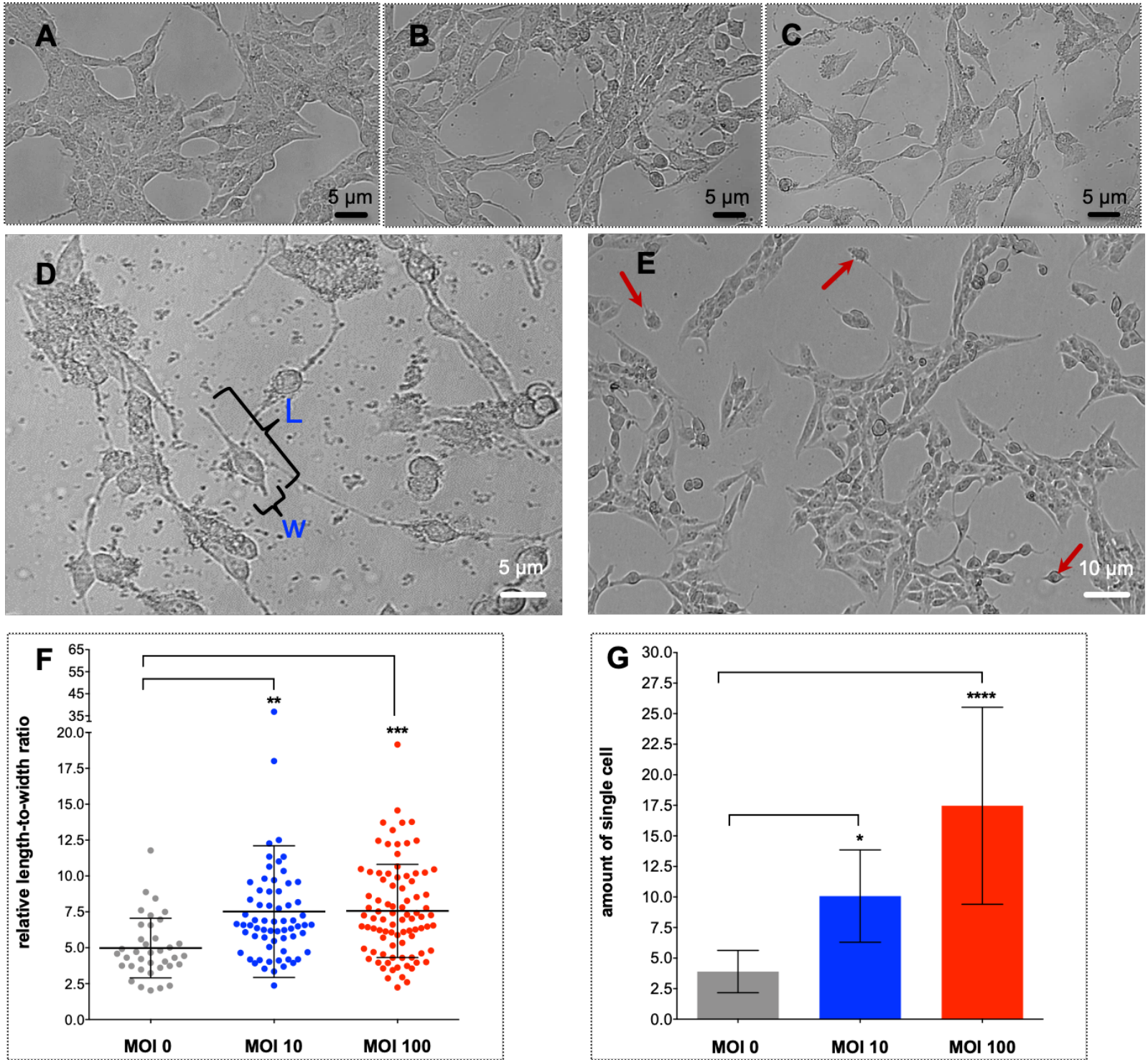
A
5 µm
B
5 µm
C
5 µm
D
L
W
5 µm
E
10 µm
F
relative length-to-width ratio
65
55
45
35
20.0
17.5
15.0
12.5
10.0
7.5
5.0
2.5
0.0
**
***
MOI 0
MOI 10
MOI 100
G
amount of single cell
30.0
27.5
25.0
22.5
20.0
17.5
15.0
12.5
10.0
7.5
5.0
2.5
0.0
*
****
MOI 0
MOI 10
MOI 100

Figure 2

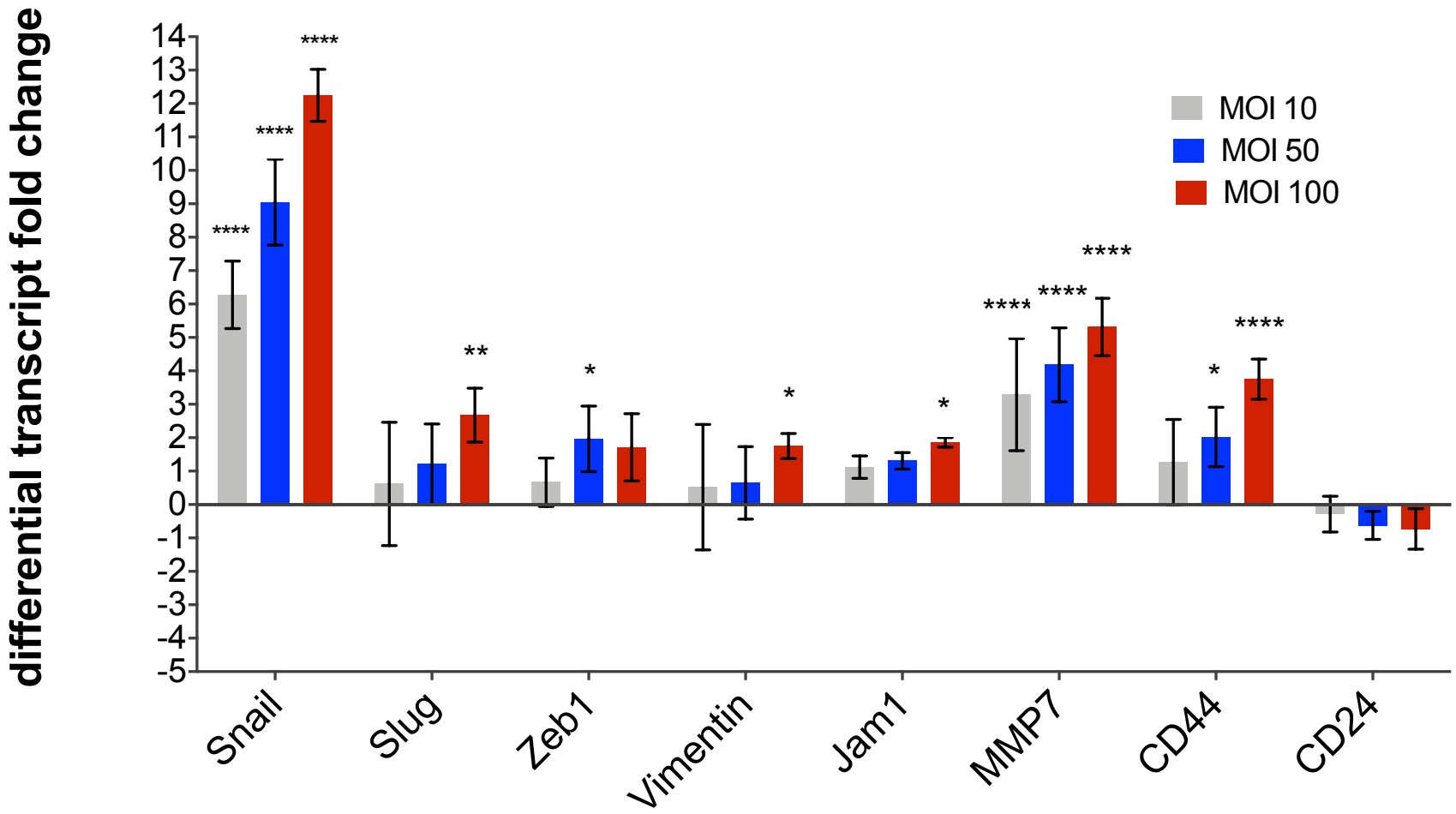
differential transcript fold change
14
13
12
11
10
9
8
7
6
5
4
3
2
1
0
-1
-2
-3
-4
-5
MOI 10
MOI 50
MOI 100
****
****
****
**
*
*
*
****
****
****
*
****
Snail
Slug
Zeb1
Vimentin
Jam1
MMP7
CD44
CD24

Figure 3

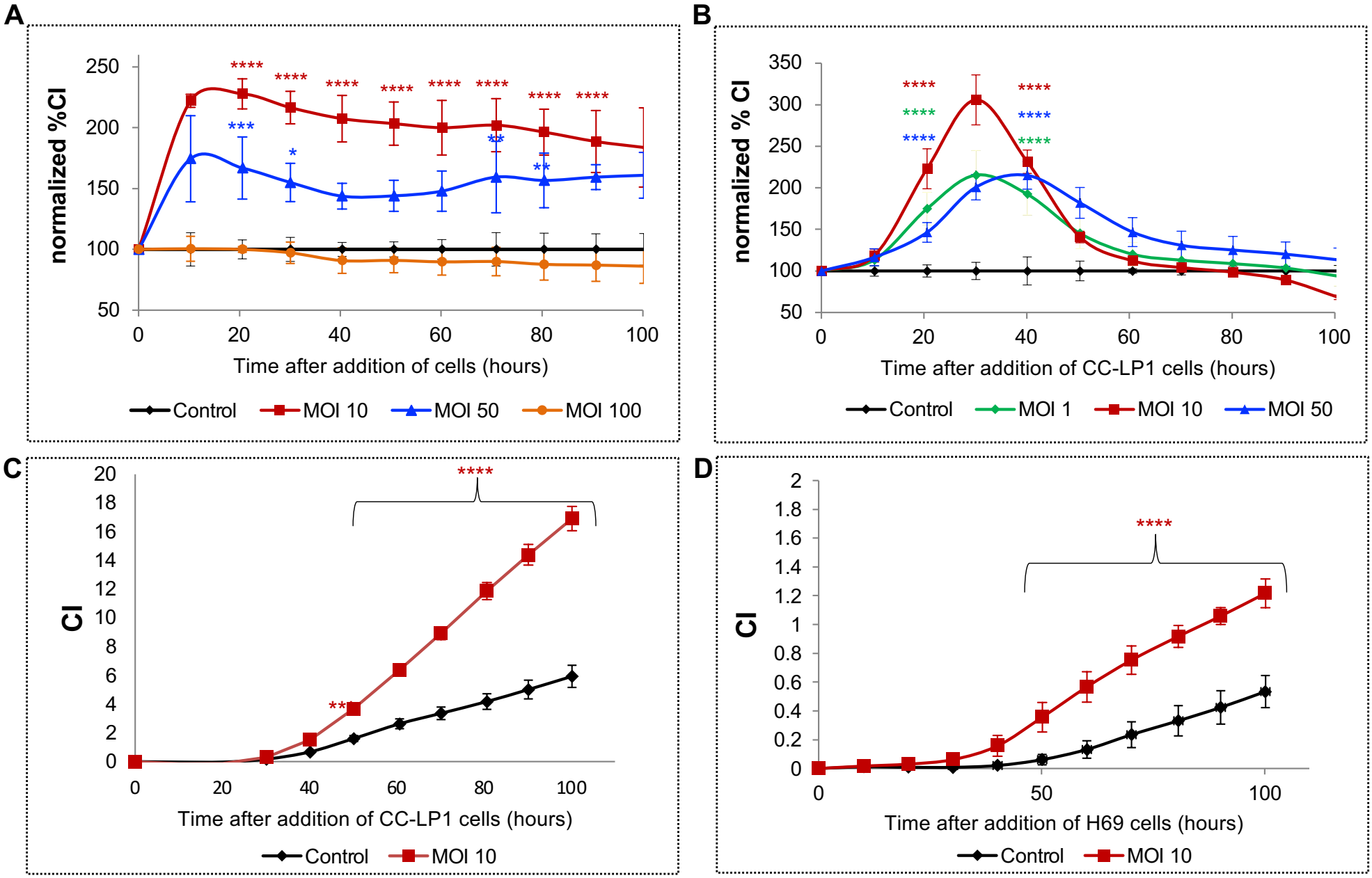
A
normalized %CI
250
200
150
100
50
0
20
40
60
80
100
Time after addition of cells (hours)
Control
MOI 10
MOI 50
MOI 100
B
normalized % CI
350
300
250
200
150
100
50
Time after addition of CC-LP1 cells (hours)
Control
MOI 1
MOI 10
MOI 50
C
CI
20
18
16
14
12
10
8
6
4
2
0
Time after addition of CC-LP1 cells (hours)
Control
MOI 10
D
CI
2
1.8
1.6
1.4
1.2
1
0.8
0.6
0.4
0.2
0
50
Time after addition of H69 cells (hours)
Control
MOI 10

Figure 4

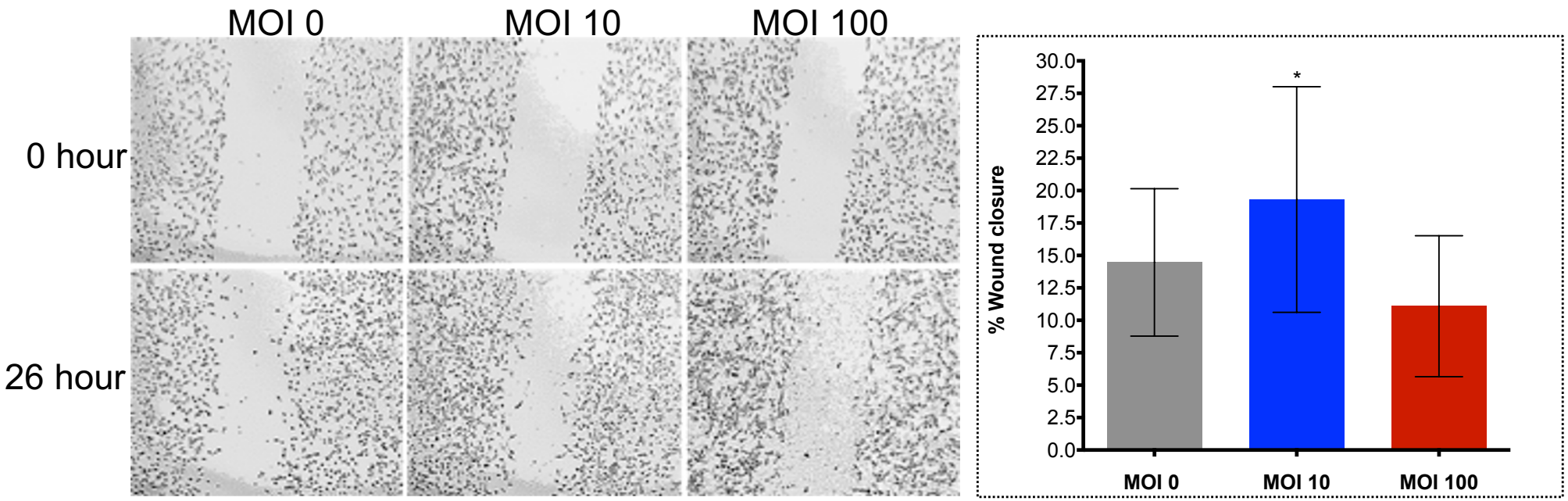
MOI 0
MOI 10
MOI 100
0 hour
26 hour
% Wound closure
30.0
27.5
25.0
22.5
20.0
17.5
15.0
12.5
10.0
7.5
5.0
2.5
0.0
*
MOI 0
MOI 10
MOI 100

Figure 5

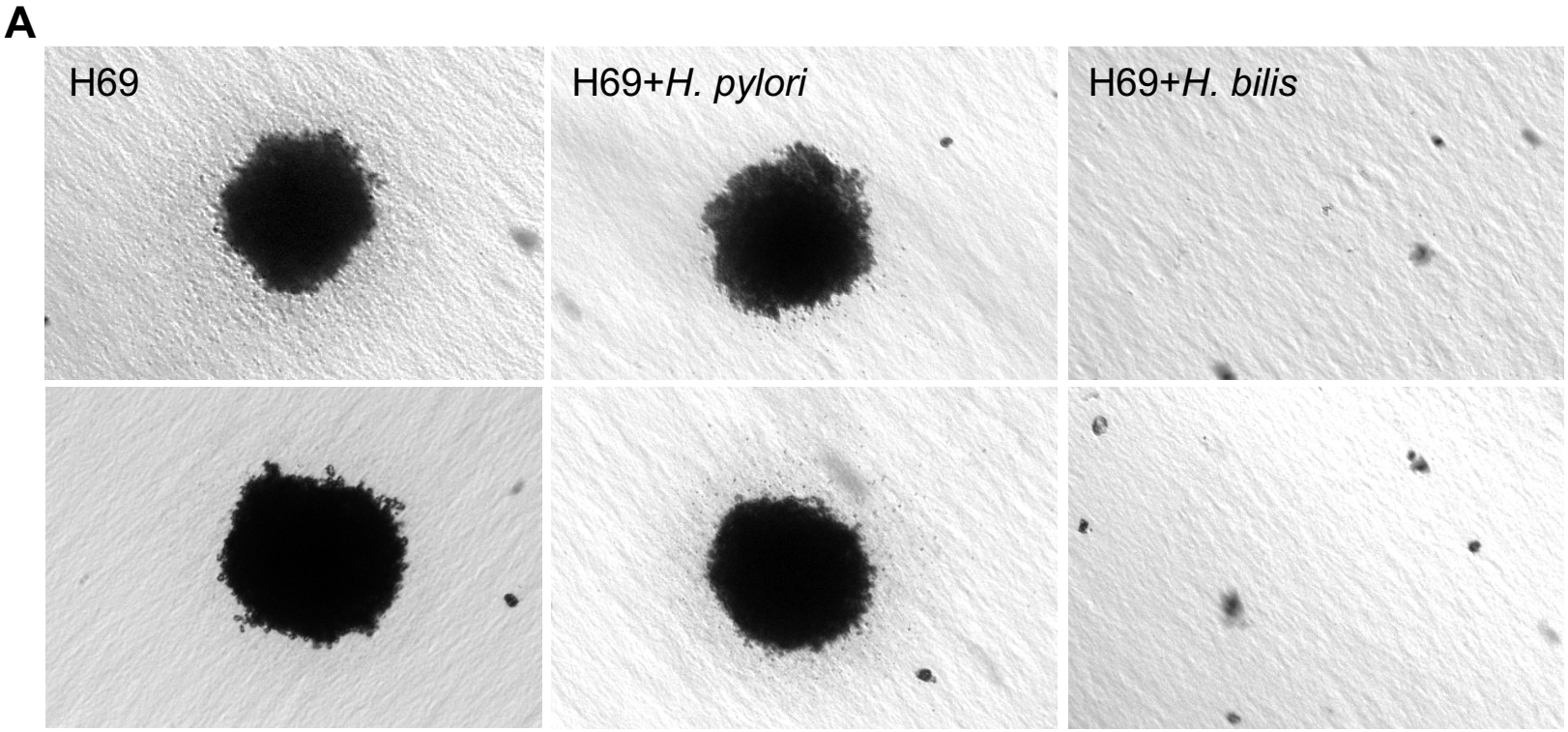
A
H69
H69+*H. pylori*
H69+*H. bilis*

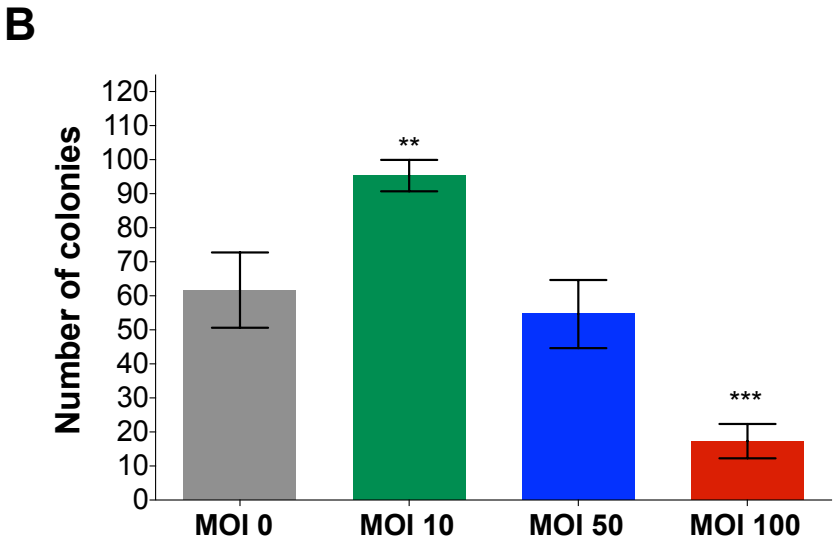
B
Number of colonies
120
110
100
90
80
70
60
50
40
30
20
10
0
**
***
MOI 0
MOI 10
MOI 50
MOI 100

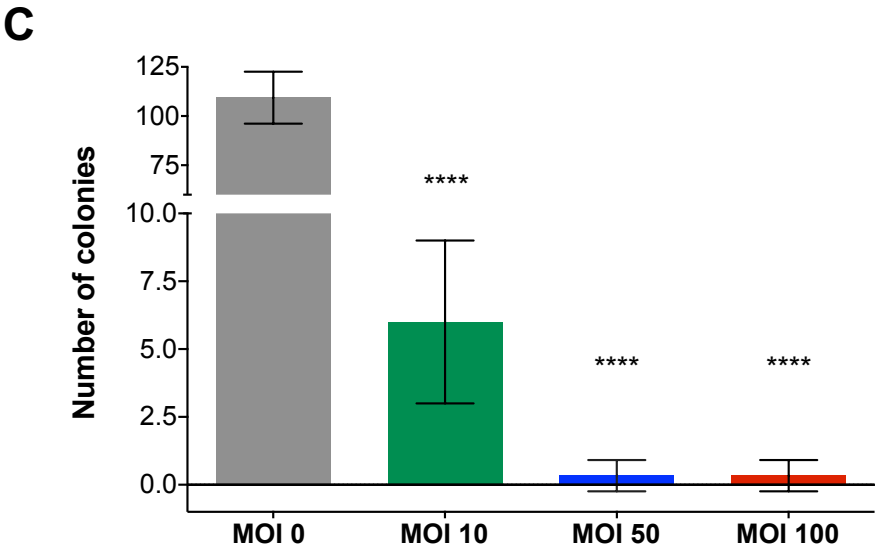
C
Number of colonies
125
100
75
10.0
7.5
5.0
2.5
0.0
****
****
****
MOI 0
MOI 10
MOI 50
MOI 100

Figure S1

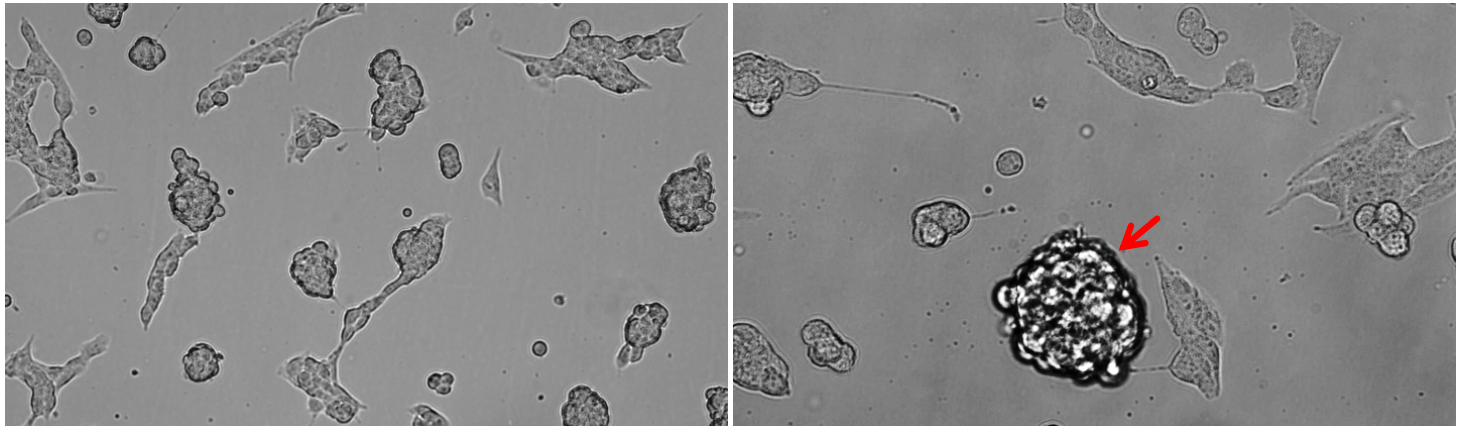

Figure S2

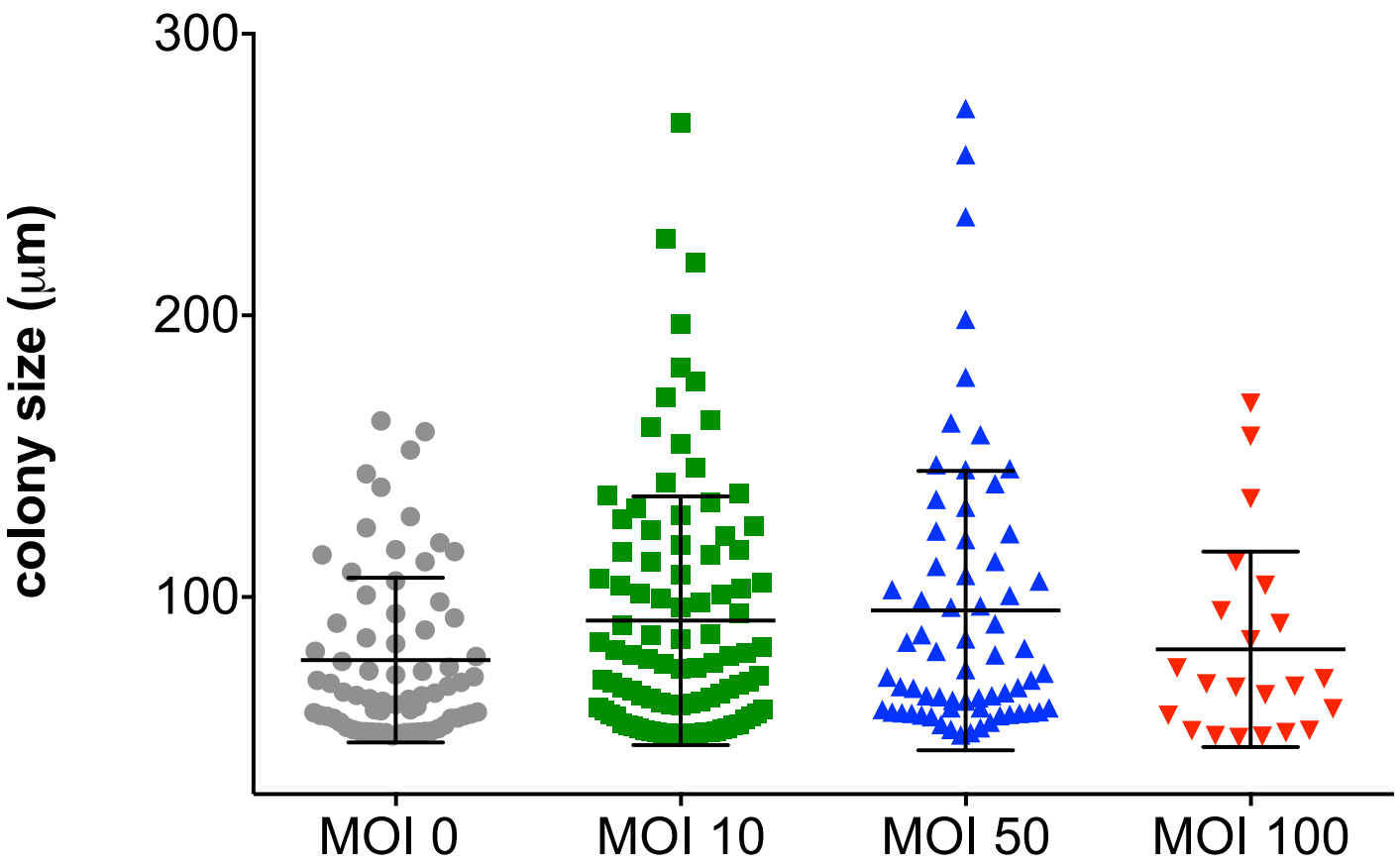

Figure S3

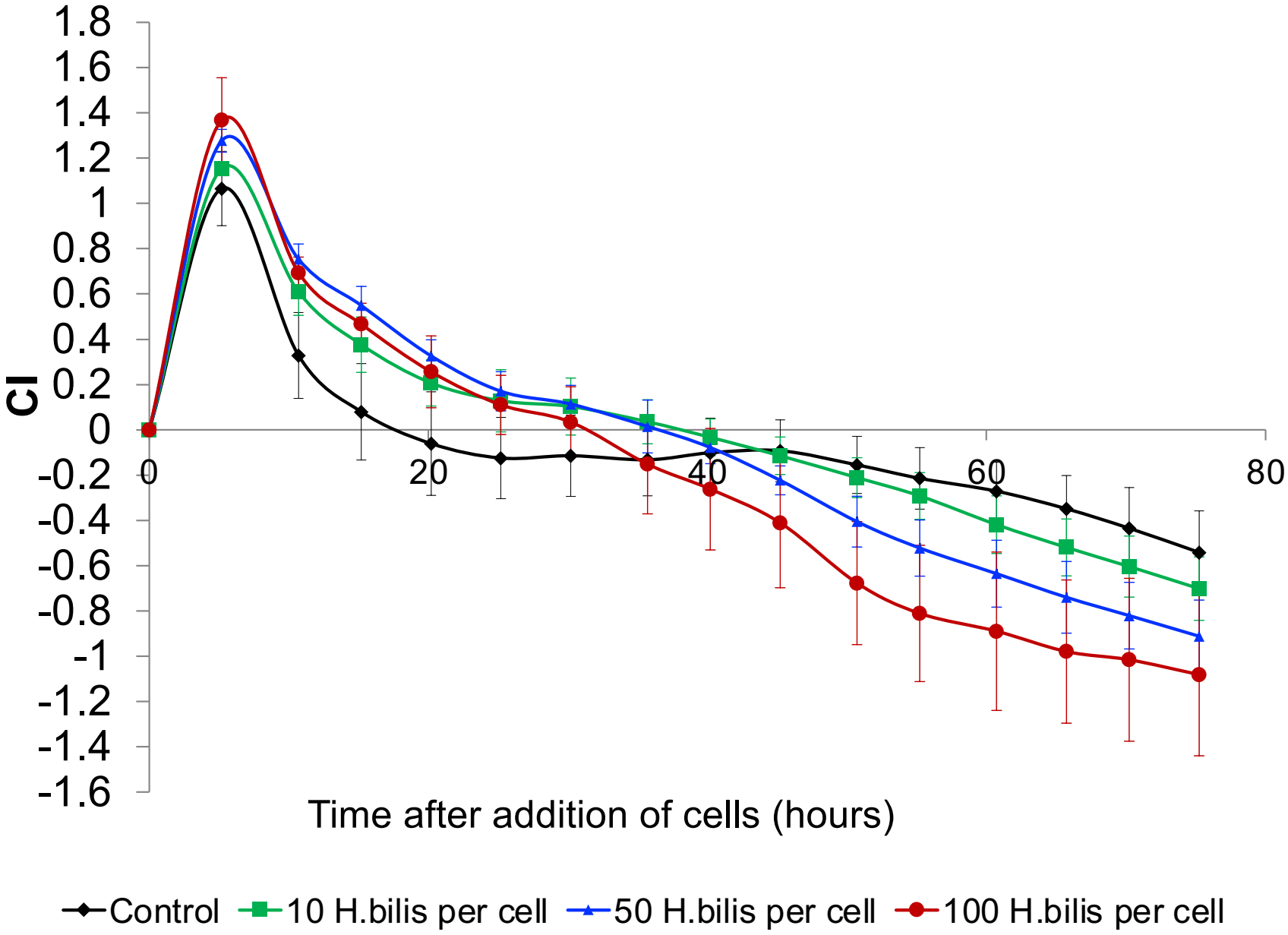
1.8
1.6
1.4
1.2
1
0.8
0.6
0.4
0.2
0
-0.2
-0.4
-0.6
-0.8
-1
-1.2
-1.4
-1.6
CI
0
20
40
60
80
Time after addition of cells (hours)
Control
10 H.bilis per cell
50 H.bilis per cell
100 H.bilis per cell